ADVANCED MATERIALS

Supporting Information

for *Adv. Mater.,* DOI: 10.1002/adma.201102277

Liquid-Crystalline Elastomer Microvalve for Microfluidics

*Antoni Sánchez-Ferrer , * Tamás Fischl , Mike Stubenrauch , Arne Albrecht , Helmut Wurmus , Martin Hoffmann , and Heino Finkelmann*

Submitted to ADVANCED MATERIALS

Supporting Information

Liquid-Crystalline Elastomer Microvalve for Microfluidics

Antoni Sánchez-Ferrer,* Tamás Fischl, Mike Stubenrauch, Arne Albrecht,
Helmut Wurmus, Martin Hoffmann, Heino Finkelmann

_____

A. Sánchez-Ferrer
Food & Soft Materials Science Group, Institute of Food, Nutrition & Health, ETH Zurich,
Schmelzbergstrasse 9, 8092 Zurich, Switzerland
Fax: +41 44 632 1603; E-mail: antoni.sanchez@agrl.ethz.ch

A. Sánchez-Ferrer, H. Finkelmann
Albert Ludwigs University, Institute for Macromolecular Chemistry, Stefan-Meier-Str. 31,
79104 Freiburg, Germany

T. Fischl, M. Stubenrauch, A. Albrecht, H. Wurmus, M. Hoffmann
Ilmenau University of Technology, Faculty of Mechanical Engineering,
Department of Micromechanical Systems, Max-Planck-Ring 14, 98693 Ilmenau, Germany

_____

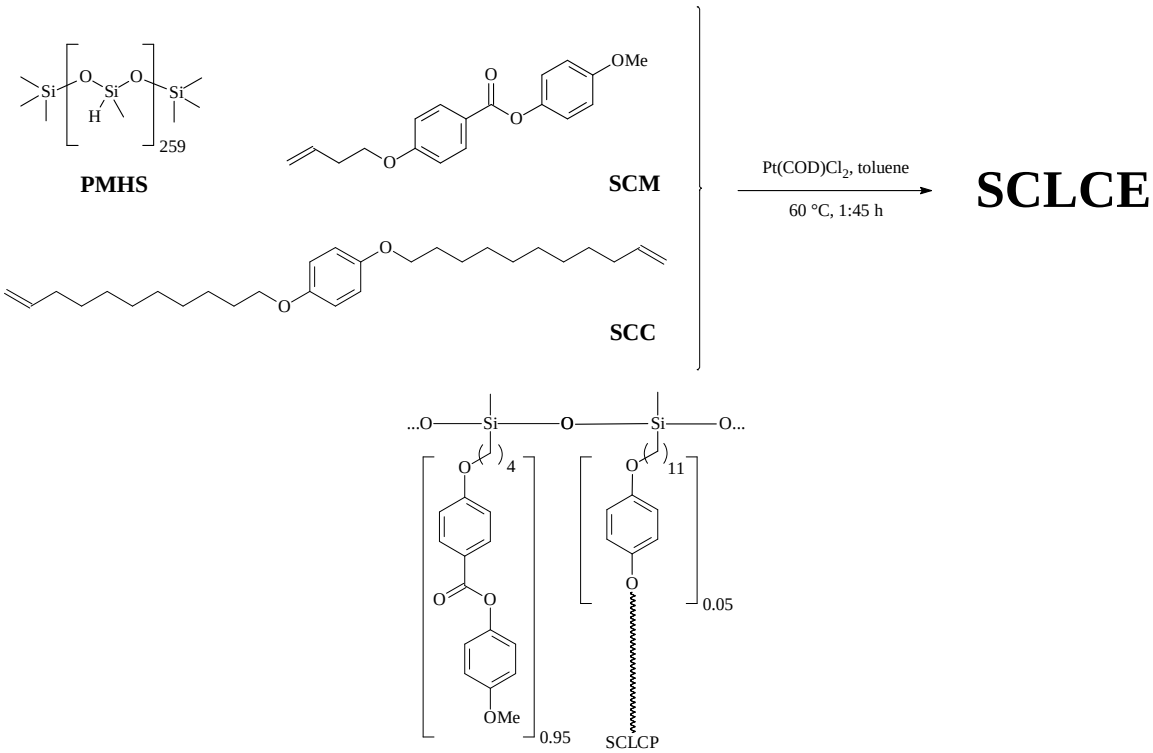

Scheme SI-1. Synthetic route for the nematic side-chain liquid-crystalline elastomer SCE-5.

Synthesis of the Mesogen and Crosslinker

The rod-like side-chain mesogen (SCM) and the isotropic side-chain crosslinker (SCC) were synthesized as described in previous papers.[I-IV]

Synthesis of the Nematic Side-Chain Liquid-Crystalline Elastomer

The orientated nematic LCE was prepared using the spin-casting technique.[IV] After the non-complete hydrosilylation reaction,[V-VIII] the sample was removed from the reactor and aligned by applying a uniaxial stress. The curing process allowed the completion of the hydrosilylation reaction, while maintaining the alignment of the sample – second step crosslinking reaction in the nematic phase during the orientation of the samples. The nematic LCE was synthesized using a 10 mol-% of crosslinking double bonds or 5.3 mol-% of crosslinker (Scheme SI-1). For this crosslinking composition, the sample has 36 side-chain repeating units between two crosslinkers.

In a 5 mL flask, 269 mg (0.90 mmol) of the side-chain mesogen (SCM) 4-methoxyphenyl 4-(but-3-en-1-yloxy)benzoate, 21 mg (0.05 mmol) of the isotropic side-chain crosslinker (SCC) 1,4-bis(undec-10-en-1-yloxy)benzene, and 60 mg (1.00 mmol SiH) of poly(methylhydrosiloxane) (PMHS, *DP* = 259) were placed. To this mixture, 1 mL of tiophene-free toluene and 20 µL of 1 %-Pt cyclooctadieneplatinum(II) chloride, $Pt(COD)Cl_2$, in dichloromethane were added. The mixture was placed in the spinning Teflon cell form which was heated at 60 °C for 1 h 45 min at 5000 rpm.

Afterwards, the reactor was cooled and the elastomer was removed from the wall. Some loads were applied in order to align the sample during the deswelling process. In this first step the elastomer is not totally crosslinked. In order to fix this orientation, the crosslinking reaction was completed by leaving the elastomer in the oven under vacuum at 60 °C for 2 days.

DSC (10 $K \cdot min^{-1}$, N_2): T_g 3 (0.45) *N* 82 (1.2) *I*; X-ray: $S = 0.73$, $d_m = 4.3$ Å; Swelling: $q = 5.6$, $q_z = 2.02$, $\alpha_z = 1.11$, $\alpha_{xy} = 2.24$

X-ray measurements showed that this nematic sample was well oriented and with a value of the order parameter of 0.73 and distance between mesogenic units of 4.3 Å (Figure SI-1). Thermoelastic experiments were performed for the determination of the anisotropic change in length during the heating and cooling process, and they showed a clearing temperature of 80.5 °C (Figure SI-2). Uniaxial stress-strain experiments were performed in the nematic phase, close to the clearing temperature, and in the isotropic state (Figure SI-3). The elastic modulus decreased when approaching the nematic-to-isotropic temperature, and increased in the isotropic state.

Apparatus and Techniques

X-ray scattering experiments were performed using a Philips PW 1730 rotating anode (4 kW) in order to obtain direct information on the WAXS reflections in the nematic phase. Cu K_α radiation (1.5418 Å) filtered by a graphite monochromator and collimated by a 0.8 mm collimator was used. The incident beam was normal to the surface of the film. The scattered X-ray intensity was detected by a Schneider image plate system (700 x 700 pixels, 250 μm resolution). The sample was placed in a self-constructed holder where temperature was controlled by a Haake-F3 thermostat. From the WAXS intensities, the mesogen distance (d_m) and the mesogen angle (ϕ) were calculated using a Gaussian distribution, and the order parameter ($S = S_d \cdot S_N$) was determined according to Lovell and Mitchell,[IX,X] where S_d is the director order parameter and S_N the order parameter that refers to the local orientational order parameter. For samples having a macroscopically uniform alignment of the director we assume that $S_d \approx 1$.

Uniaxial stress-strain measurements were performed with a self-constructed apparatus. In a cell controlled by a Haake-F6 thermostat and equipped with a Pt100 thermoresistor, the sample was stretched by one Owis SM400 microstep motor and controlled by an Owis SMK01 microstep controller. The stress (σ) was measured by a HBM PW4FC3 transducer load cell (300 g) and analyzed by an HBM KW3073 high-performance strain gauge indicator. All relevant data such as temperature, uniaxial strain ($\lambda = L/L_0$) and uniaxial stress (σ) were continuously logged. A personal computer controlled the deformation stepwise as specified by a script file. After each deformation step, the static response to the deformation, the uniaxial stress (σ) was recorded once equilibrium was reached according to the slope and the standard deviation of the continuously logged data.

Thermoelastic measurements were performed with a self-constructed apparatus designed to measure the length of the elastomer as function of temperature. The sample was mounted in a thermostated glass column. The change in length ($\lambda = L/L_{ISO}$) was recorded by a Canon Power Shot A520 Digital Camera. Temperature was continuously logged and controlled by a Haake-F6 thermostat and measured with a Pt100 thermoresistor. A personal computer controlled the temperature stepwise as specified by a script file. After each temperature step, uniaxial expansion (cooling) or contraction (heating) were recorded when thermal equilibrium was reached according to the slope and the standard deviation of the continuously logged data. Afterwards, pictures were evaluated by image processing in order to calculate the change in length at each temperature.

Microvalve Characterization

An electric thermoresistor (Pt100) was connected to a full Wheatstone-bridge in order to measure the temperature on the microchip. The cooper electrical circuit (R_{heat} = 30 Ω) was powered through an electronic control with the help of a power supply (DC 30 V), and monitored with a data acquisition card (DAQ card, Labjack U12). The microfluidic channels were branched before and after the microchip, and a pressure sensor measured the differential pressure on the microvalve. Liquid-phase medium (water) was used for the characterisation of the system because water has higher specific heat capacity than gases. A water reservoir of 1.5 L was hung up in a defined height above the valve (for example z_0 = 0.172 m; p_0 = 1.69 kPa) to generate a pulse-free flow for the microvalve ranging from 80 to 300 μL·s^{-1}. The water was collected in a reservoir in order to measure the volumetric flow rate. The controlling software increased the voltage linearly ($\Delta U_{control}/\Delta t$ = 125 mV·s^{-1}), which raised the heating power on the microvalve until reaching the maximum temperature of T_{max} = 85 °C of the LCE and closing the microvalve. The controlling voltage was switched off when the temperature reached to the maximum. Afterwards, the cooling process started, and the microvalve opened when the temperature fell below the closing point. The opening of the microvalve depends on the applied pressure and happens on a defined temperature (Scheme SI-2).

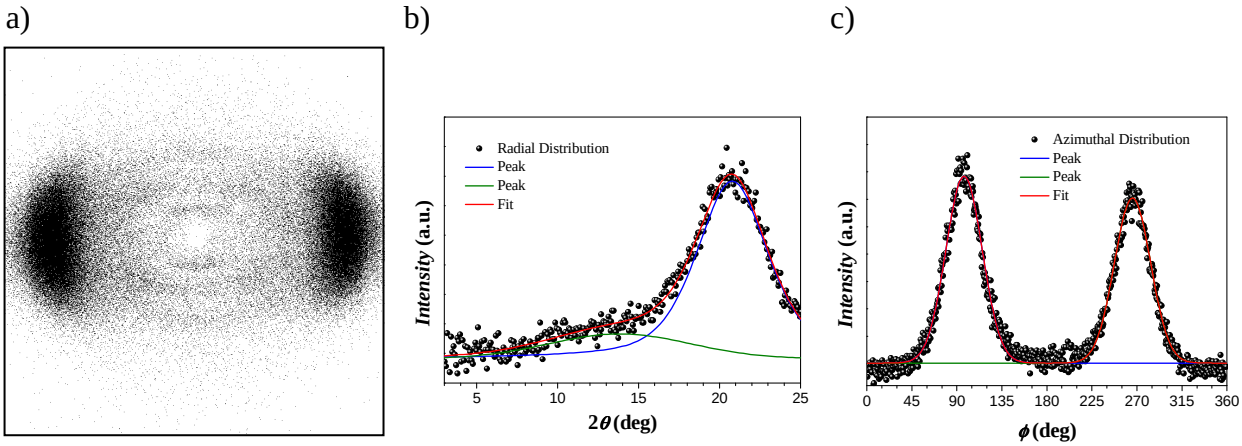

Figure SI-1. a) 2D WAXS scattering pattern, b) radial distribution, and c) azimuthal distribution of the nematic side-chain liquid-crystalline elastomer SCE-5.

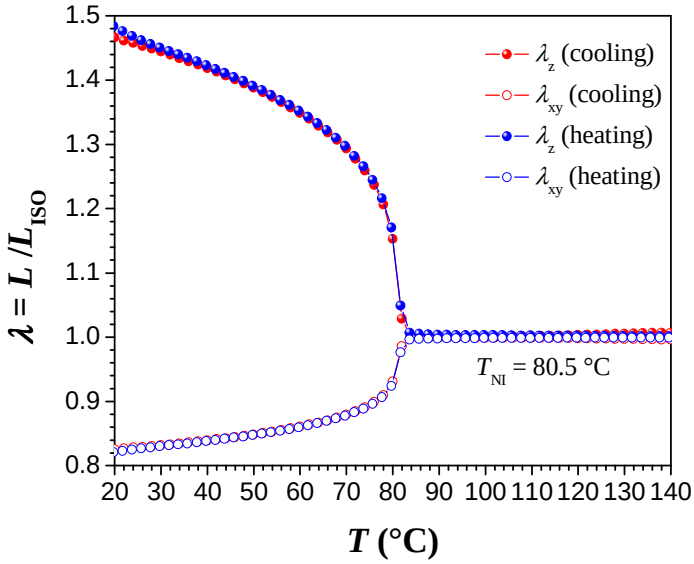

Figure SI-2. Thermoelastic curves during the cooling and heating process for the nematic side-chain liquid-crystalline elastomer SCE-5.

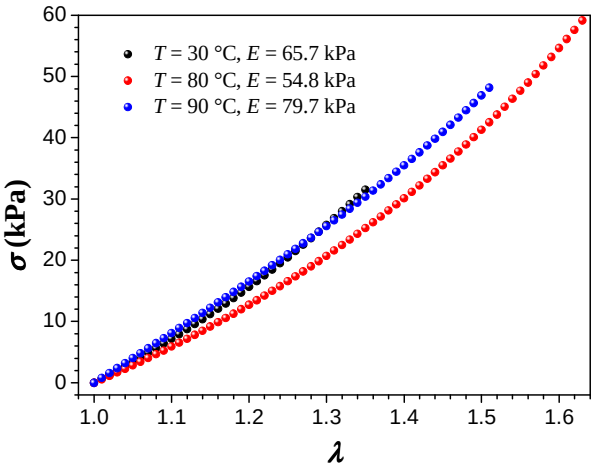

Figure SI-3. Uniaxial stress-strain curves for the nematic side-chain liquid-crystalline elastomer SCE-5 in the nematic phase (T = 30 ºC), in the nematic-to-isotropic transition (T = 80 ºC), and in the isotropic phase (T = 90 ºC).

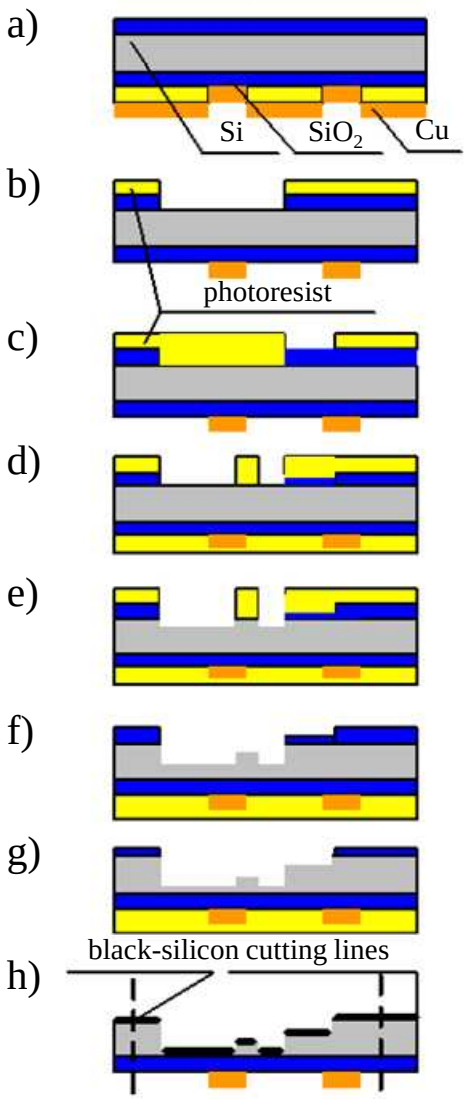

Figure SI-4. Multi-step photolithography process with subsequent etchings of the SiO_2 (wet or dry etching) for the manufacturing of the microchip.

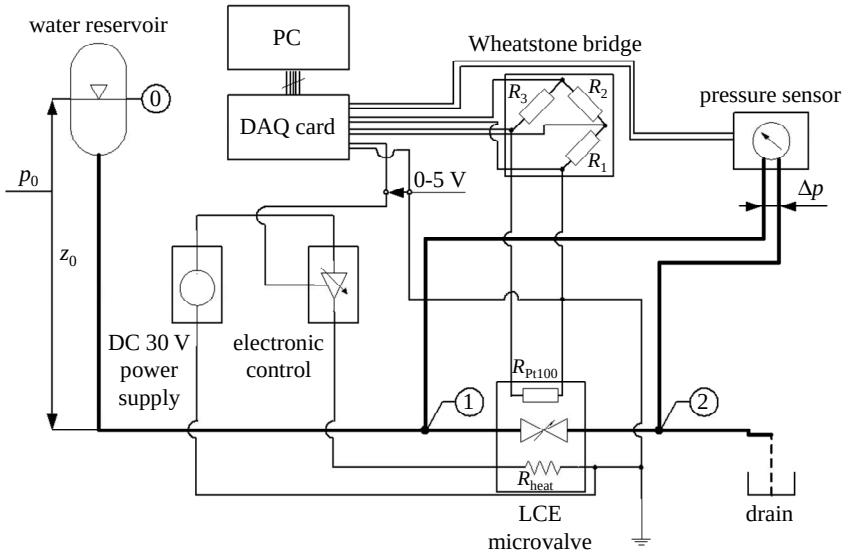

Scheme SI-2. Schematic measurement principle for the characterization of the LCE microvalve.

References

[I] H. Finkelmann, U. Kiechle, G. Rehage, *Mol. Cryst. Liq. Cryst.* **1983**, *94*, 343.

[II] J. Küpfer, H. Finkelmann, *Makromol. Chem. Rapid Commun.* **1991**, *12*, 717.

[III] J. Küpfer, H. Finkelmann, *Macromol. Chem. Phys.* **1994**, *195*, 1353.

[IV] H. Finkelmann, A. Greve, M. Warner, *Eur. Phys. J. E* **2001**, *5*, 281.

[V] J. Yoshida, K. Tamao, M. Takahashi, M. Kumada, *Tetrahedron Lett.* **1978**, *25*, 2161.

[VI] W. Caseri, P.S. Pregosin, *Organometallics* **1988**, *7*, 1373.

[VII] B. Marciniec, *"Comprehensive Handbook on Hydrosilylation"*, Pergamon, Oxford, 1992.

[VIII] N. Sabourault, G. Mignani, A. Wagner, C. Mioskowski, *Org. Lett.* **2002**, *4*, 2117.

[IX] Lovell, R.; Mitchell, G. R. *Acta Crystallogr. A* **1981**, *37*, 135.

[X] Mitchell, G. R.; Windle, A. H. In *Development in Crystalline Polymers-2*; Basset, D. C., Ed.; Elsevier Applied Science: London, 1988; Vol. 3, p 115.